Axial Load Tests of Concrete Compression Members with High Strength Spiral Reinforcement

Stephen Pessiki, Ph.D.
Associate Professor
Department of Civil and Environmental Engineering
Lehigh University,
Bethlehem, Pennsylvania

Benjamin A. Graybeal
Research Engineer
Wiss, Janney, Elstner Associates, Inc.
FHWA NDE Validation Center
McLean, Virginia

Axial load tests were performed to evaluate the confinement effectiveness of high strength spiral reinforcement in concrete compression members. The tests included 24 and 14 in. (610 and 356 mm) diameter circular cross section compression members with spiral nominal yield strengths that ranged from 78 to 140 ksi (538 to 965 MPa). It was found that while spiral steel stresses in excess of 60 ksi (414 MPa) are achieved, the nominal yield strength of the spiral may not be achieved. The stress reached in the spiral depends in part upon the compression member diameter, with smaller diameter members able to reach a greater fraction of the nominal yield strength as compared to the larger diameter members. For a given concrete cover thickness, these smaller diameter members have a greater volume fraction of spiral reinforcement as compared to larger diameter members. Compression members made with high strength spirals exhibit the same ductile axial load-axial shortening behavior expected from members made with mild steel spirals.

Spiral reinforcement as used in a compression member produces a state of triaxial compression by restraining the lateral expansion of the concrete as the member is compressed axially. The lateral confinement created by the spiral increases both the strength and deformation capacity of the concrete.

Spiral reinforcement is often used as transverse reinforcement in compression members such as columns and precast, prestressed concrete piles. Spiral reinforcement is proportioned in part based on the concrete compressive strength. In short, spiral reinforcement is designed so that, in the event that the compression member is overloaded, the spiral provides enough strength enhancement to the core concrete to replace the strength lost as the cover concrete spalls away.

For a given compression member cross-sectional geometry, a higher compressive strength concrete requires a greater volume fraction of

spiral reinforcement. Thus, as concrete strengths have increased over the years, the amount of spiral reinforcement required has increased as well.

This increased amount of spiral reinforcement is provided through the use of a larger diameter spiral bar and/or through smaller pitch. This can create a problem during fabrication in that a small pitch, large diameter spiral bar can complicate concrete placement and consolidation. Additionally, restrictions on spiral pitch may be encountered based on concrete aggregate size.

One approach to minimize the reinforcement congestion problem is to increase the spiral reinforcement yield strength. Assuming that the steel has yielded, a higher yield strength spiral along with a smaller volume fraction of spiral reinforcement may be used to provide the required amount of confining stress to the concrete.

In general, present design codes limit the design yield strength of spiral reinforcement to 60 ksi (414 MPa). This limit is based on a lack of evidence that steel with a greater yield strength will achieve yield prior to the member reaching its peak strength.

OBJECTIVE AND APPROACH

The objective of this research is to evaluate the confinement effectiveness of high strength spiral reinforcement in compression members such as columns and precast, prestressed concrete piles. This paper presents the results of tests of eight large-scale spirally reinforced concrete compression members loaded in concentric axial compression. The tests included two compression member diameters, and the design nominal yield strength of the spiral reinforcement varied from 78 to 140 ksi (538 to 965 MPa).

The test specimens were designed according to the requirements of ACI 318 Building Code Requirements for Structural Concrete[1] and American Association of State Highway and Transportation Officials LRFD Bridge Design Specifications[2] (hereafter referred to as the ACI 318 Code and the AASHTO Design Specification, respectively). Complete details of the test program are given in Graybeal[3] and Graybeal and Pessiki.[4]

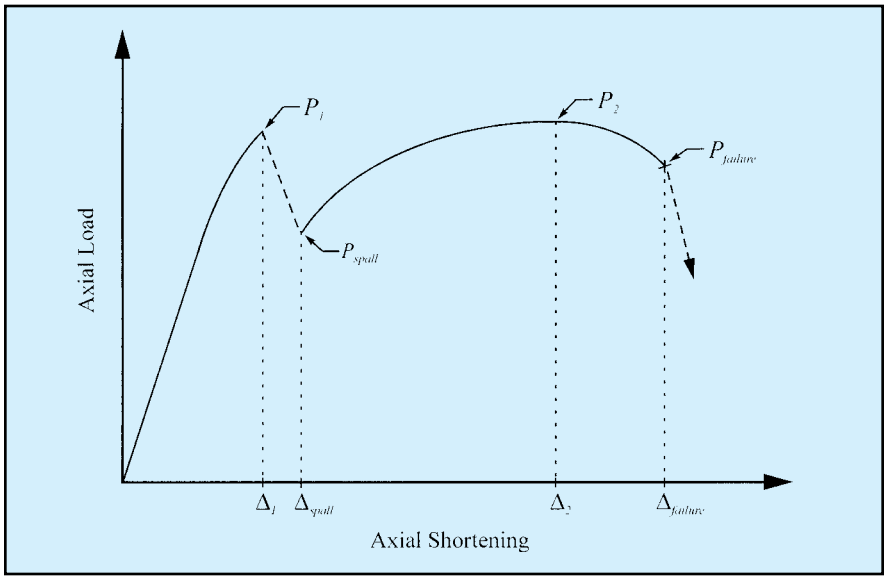

Fig. 1. Idealized axial load-axial shortening behavior of a spirally-reinforced member.

BACKGROUND

The general behavior of spirally reinforced concrete compression members has been thoroughly studied and documented over the past century. In the early 1900s, Considère[5] found that the compressive strength of concrete could be increased if a transverse confining pressure was applied. This confining pressure, whether active (i.e., applied externally by a pressurized fluid) or passive (i.e., created by lateral expansion of the axially compressed concrete against a confining material), worked to resist the lateral expansion of concrete as it was loaded axially.

Richart, Brandzaeg, and Brown[6-8] presented an equation of the following form to describe the relationship between the unconfined concrete compressive strength f_{co}, lateral pressure $f_{2\text{-}2}$, and the confined concrete compressive strength f_{c2}:

$$f_{c2} = f_{co} + 4.1 f_{2-2} \qquad (1)$$

Richart et al. also proposed the following equation which relates the strain at the peak compressive strength, ε_{c2}, to the peak compressive strength, f_{c2}, the unconfined compressive strength, f_{co}, and the corresponding unconfined strain, ε_{co}:

$$\varepsilon_{c2} = \varepsilon_{co}\left(5\frac{f_{c2}}{f_{co}} - 4\right) \qquad (2)$$

Fig. 1 shows the idealized axial load-axial shortening behavior of a spirally reinforced concrete compression member. Several key load and shortening values in the response are indicated in the figure. Loads P_1, P_{spall}, P_2, and $P_{failure}$ indicate the loads at the initiation of cover loss, the conclusion of cover loss, the confined peak, and the failure of the member (defined by fracture of the spiral reinforcement), respectively. Displacements Δ_1, Δ_{spall}, Δ_2, and $\Delta_{failure}$ indicate the axial shortening values at the corresponding loads.

A concrete member without spiral reinforcement exhibits a load capacity approximately equal to P_1, and a continuous decrease in resistance with an increase in applied deformation beyond that point. Fig. 1 shows that the presence of spiral reinforcement leads to a second peak in the response, and that this second peak is reached at a much greater axial shortening than is achieved by an unconfined member.

CURRENT DESIGN CODE REQUIREMENTS

Requirements for the design of spirally reinforced compression members (such as columns and piles) are given in the ACI 318 Code and AASHTO Design Specification.

The ACI 318 Code and the AASHTO Design Specification both state

that the nominal concentric axial load capacity, P_o, of an axially loaded non-prestressed member is given by:

$$P_o = 0.85 f_{co}\left(A_g - A_{st}\right) + A_{st} f_y \quad (3)$$

where

A_g = gross cross-sectional area of the compression member
A_{st} = area of the longitudinal reinforcement
f_y = yield strength of the longitudinal reinforcement

The Precast/Prestressed Concrete Institute Industry Design Handbook[9] (hereafter referred to as the PCI Handbook) provides a similar equation, except that it takes into account the prestress force present within a prestressed member through the equation:

$$P_o = \left(0.85 f_{co} - 0.60 f_{pc}\right) A_g \quad (4)$$

where f_{pc} is the concrete compressive stress due to the effective prestress.

The volumetric ratio of spiral reinforcement in a compression member, defined as the ratio of the volume of the spiral to the volume of the concrete core, is computed as:

$$\rho_{sp} = \frac{4 A_{sp}}{d_{sp} s} \quad (5)$$

where the spiral wire cross-sectional area, pitch, and out-to-out diameter are A_{sp}, s, and d_{sp}, respectively.

The confining pressure $f_{2\text{-}2}$ which is applied to the concrete core by spiral reinforcement can be calculated as:

$$f_{2-2} = \frac{1}{2} \rho_{sp} f_{sp} \quad (6)$$

where ρ_{sp} is the volumetric ratio of spiral reinforcement and f_{sp} is the stress in the spiral reinforcement.

Spiral reinforcement is designed according to the philosophy that the strength reduction caused by spalling of the concrete cover should equal the strength gain of the concrete core due to confinement. In equation form, this is written as:

$$0.85 f_{co}\left(A_g - A_{core}\right) = 4.1 f_{2-2} A_{core} \quad (7)$$

where A_{core} is the area of the concrete core.

Substituting Eq. (6) and solving for ρ_{sp} leads to:

$$\rho_{sp} = 0.42 \frac{f_{co}}{f_{sp}}\left(\frac{A_g}{A_{core}} - 1\right) \quad (8)$$

In the design codes, the 0.42 factor is increased slightly to 0.45, and the required amount of spiral reinforcement is given as:

$$\rho_{sp} \geq 0.45 \frac{f_{co}}{f_{sy}}\left(\frac{A_g}{A_{core}} - 1\right) \quad (9)$$

In Eq. (9), the stress in the spiral reinforcement, f_{sp}, is assumed to equal f_{sy}, the yield strength of the spiral reinforcement. Compression members designed using Eq. (9) are expected to

(a)

(b)

Fig. 2. Reinforcing cages (spiral strengths A-D from left to right): (a) 10 in. (254 mm) diameter cage; (b) 20 in. (508 mm) diameter cage.

exhibit the idealized behavior shown in Fig. 1.

In the derivation above, the spiral reinforcement is assumed to act at its yield stress when Δ_2 is reached. However, in order to ensure sufficient confinement, an upper limit of f_{sy} = 60 ksi (414 MPa) is placed on the yield strength of the spiral reinforcing steel. Through this means, the volumetric ratio of transverse reinforcement remains high and the confining pressure at the second peak is very likely at or above the expected level.

EXPERIMENTAL PROGRAM

This section of the paper describes the experimental program. As noted earlier, complete details of the program are given in Graybeal[3] and Graybeal and Pessiki.[4]

Test Matrix

The test matrix, presented in Table 1, includes a total of eight compression member specimens. The primary variables treated were compression member diameter and spiral yield strength. Table 1 includes an alphanumeric identifier for each specimen. The prefixes '24' and '14' refer to specimens with 24 and 14 in. (610 and 356 mm) diameters, respectively, and the 'A', 'B', 'C', and 'D' are used to denote the nominal spiral steel yield strengths as follows: A = 78 ksi (538 MPa); B = 107 ksi (738 MPa); C = 121 ksi (834 MPa); and D = 140 ksi (965 MPa), respectively. These nominal yield strength values were provided by the spiral manufacturer.

Specimen Details

Table 1 also summarizes the details of each specimen. The 24 in. (610 mm) diameter specimens all measured 96 in. (2.44 m) in height and the 14 in. (356 mm) diameter specimens all measured 56 in. (1.42 m) in height. Thus, all specimens had a height-to-diameter aspect ratio of 4 to 1. All specimens had a 2 in. (51 mm) clear concrete cover between the outside diameter of the spiral reinforcement and the outer surface of the specimen. The design concrete compressive strength was 8.0 ksi (55.2 MPa).

Fig. 2 shows the completed reinforcement cages. As shown in the figure, the portion of each specimen within one diameter of height from each end was provided with extra spiral reinforcement to increase the confinement in these end regions. The test region was defined as the section of the specimen which was between the more heavily confined end regions.

Within each test region, the spiral reinforcement was proportioned according to the ACI 318 Code and AASHTO Specification based on the design concrete compressive strength and the manufacturer-supplied nominal spiral yield strengths as stated above. All spiral wires treated in the study had a diameter, d_{sw}, of 0.35 in. (8.89 mm).

Also, to provide additional clear spacing between spiral turns, two wires were bundled to create the spiral in the two lower spiral yield strength specimens of each diameter (14-A, 14-B, 24-A, and 24-B). This is shown in Fig. 2 and Table 1 (n_{sp} is the number of wires in the bundle). The mild longitudinal steel reinforcement shown in Table 1 was used to hold the spiral in position during fabrication.

Instrumentation

Electrical resistance strain gauges were used to monitor strains in both the spiral and longitudinal reinforcement. A total of twelve strain gauges, all placed within the test region, were used on each specimen. The general layout of the gauges on each specimen was similar to that shown for a 14 in. (356 mm) diameter specimen shown in Fig. 3.

In the specimens with bundled spirals, the gauges were located alternately on each spiral in the bundle. In addition, linear variable differential transformer (LVDT) displacement transducers were used to measure the overall axial shortening.

Table 1. Description of test specimens.

Specimen		Spiral reinforcement						Longitudinal reinforcement	
I.D.	Diameter (in.)	$f_{sy,nom}$ (ksi)	d_{sw} (in.)	n_{sp}	A_{sp} (in.^{2})	s (in.)	ρ_{sp} (percent)	Bars	ρ_{lg} (percent)
24-A	24	78	0.35	2	0.1924	1.875	2.05	6-#4	0.26
24-B	24	107	0.35	2	0.1924	2.500	1.54	6-#4	0.26
24-C	24	121	0.35	1	0.0962	1.500	1.28	6-#4	0.26
24-D	24	140	0.35	1	0.0962	1.750	1.10	6-#4	0.26
14-A	14	78	0.35	2	0.1924	1.750	4.40	4-#4	0.51
14-B	14	107	0.35	2	0.1924	2.375	3.24	4-#4	0.51
14-C	14	121	0.35	1	0.0962	1.375	2.80	4-#4	0.51
14-D	14	140	0.35	1	0.0962	1.500	2.57	4-#4	0.51

Note: 1 ksi = 6.895 MPa; 1 in. = 25.4 mm.

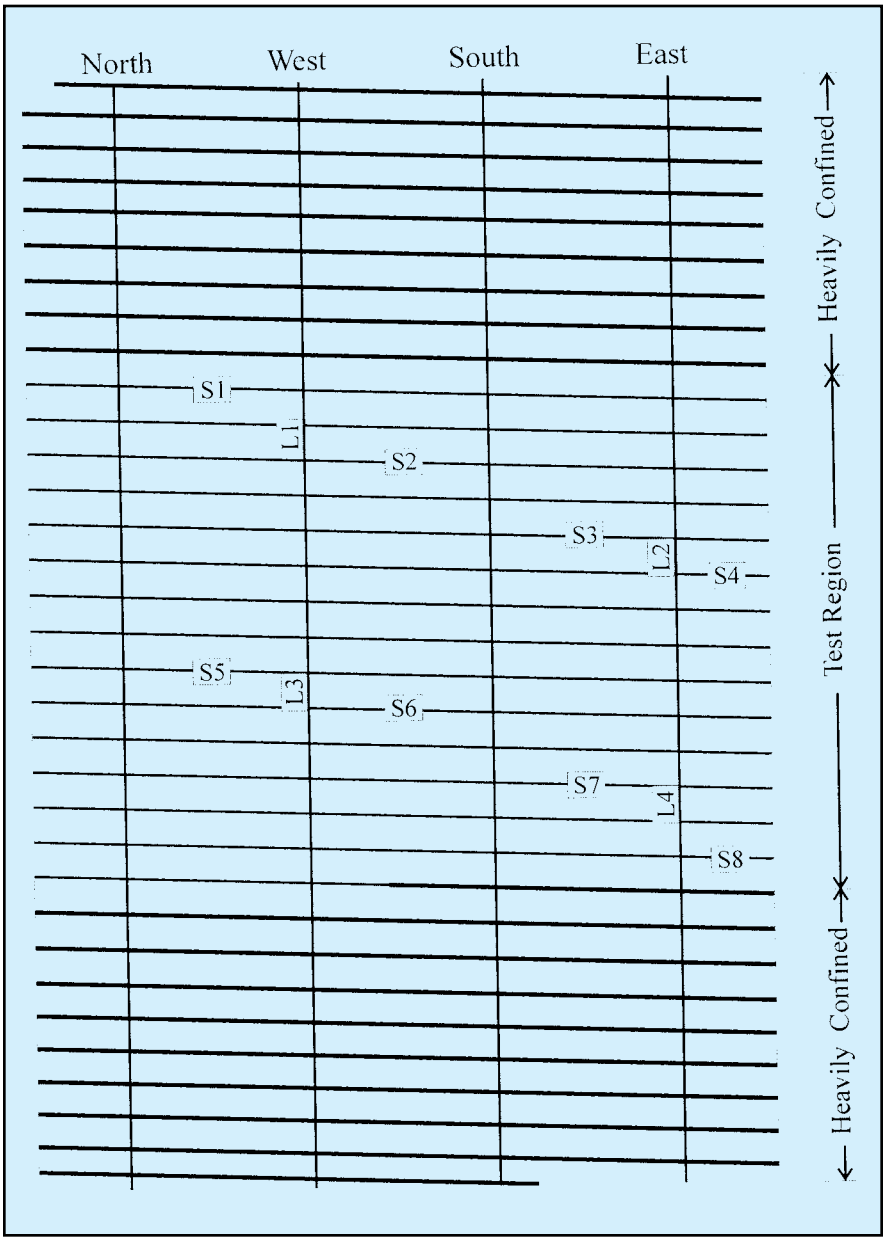

Fig. 3. Typical layout of strain gauges.

Specimen Fabrication

The reinforcement cages were produced from spirals comprised of approximately 20 to 25 turns of wire, and straight longitudinal reinforcing bars. The cages were produced in such a way that no spiral lapped spliced occurred within the test region, although every specimen did have a number of splices outside of the test region.

For each splice, the overlap of the two spirals was 1 to 1.5 turns. The ends of the spliced spirals were also bent into the confined core to aid in development of the spiral. All specimens were positioned in a vertical orientation during concrete placement.

Concrete Properties

The concrete material property of primary interest is the unconfined compressive strength. Three different approaches were used to determine this value:

First, compression tests were made on 6 x 12 in. (152 x 305 mm) field-cured cylinders cast during the concrete pour.

Second, plain concrete compression member specimens were prepared along with the eight test specimens. These plain concrete specimens were intended to have the same curing history as the reinforced test specimens. Cores 6 x 12 in. (152 x 305 mm) were cut from the plain concrete specimens and tested in compression.

Finally, the unconfined concrete compressive strength was computed from the first peak (P_1) in the axial load response of each specimen. Based on the results of all compression tests, the unconfined concrete compressive strength, f_{co}, is taken as 8.5 ksi (58.6 MPa).

The stress-strain curve of the unconfined concrete was determined from the compression tests of the field-cured and cored cylinders. From these tests, the axial concrete strain corresponding to the unconfined concrete strength, ε_{co}, was determined to be 0.0027.

Steel Properties

According to the spiral manufacturer, the spiral reinforcement treated in the study was produced through a cold-drawing process from four different grades of undeformed steel wire. Each steel wire was then turned into a spiral such that the outer cage diameter was 20 and 10 in. (508 and 254 mm), respectively, for the 24 and 14 in. (610 and 356 mm) diameter specimens. No stress-relieving was performed either before or after the wire was turned into a spiral.

The nominal yield strength values as reported by the spiral manufacturer for the four grades of spiral were 78, 107, 121, and 140 ksi (538, 738, 834, and 965 MPa). The spiral manufacturer performed material testing on the spiral wire after the drawing process, but before the wire had been turned into a spiral.

Tension tests were performed at Lehigh University on lengths of spiral wire that were cut from the 20 in. (508 mm) diameter spirals for all four grades of steel. These lengths were first straightened as much as possible by bending prior to the tension tests. Strain gauges were placed along the longitudinal axis of the wire to obtain axial strain readings.

The process of turning a steel wire into a spiral changes the mechanical properties of the steel. Specifically, spiraling causes permanent plastic deformations and residual stresses within the cross section of the wire. Therefore, a spiraled length of wire will not exhibit the same tensile stress-strain properties as a similar length of wire which was never spiraled.

Straightening a spiraled wire introduces further changes to the residual stresses within the cross section, and thus causes further changes in the tension stress-strain properties of the wire. A detailed explanation of the effects of spiraling on the stress-strain properties of the spiral reinforcement is given elsewhere.[3,4]

Fig. 4 shows the tensile stress-strain curves which were obtained from the sections of spiraled-straightened wire. For Wires B, C and D, just prior to fracture, both the stress and strain are observed to decrease. This is due to necking which occurs along the wire at a location away from where the strain gauges were located. For the Grade A spiral, necking occurred directly under the strain gauges.

Table 2 summarizes the results of tension tests for the four grades of spiral reinforcement. The yield strength is given both as reported by the spiral manufacturer and as determined from the tension testing performed at Lehigh University.

The testing method used by the spiral manufacturer is basically an elongation under load method, as described in ASTM A370. This standard is referenced from ASTM A82 which defines standards for steel wire used as concrete reinforcement. The elongation under load method is generally used for determining the tensile yield properties of a steel tensile specimen that does not exhibit a well-defined yield point.

In the Lehigh University tests, the

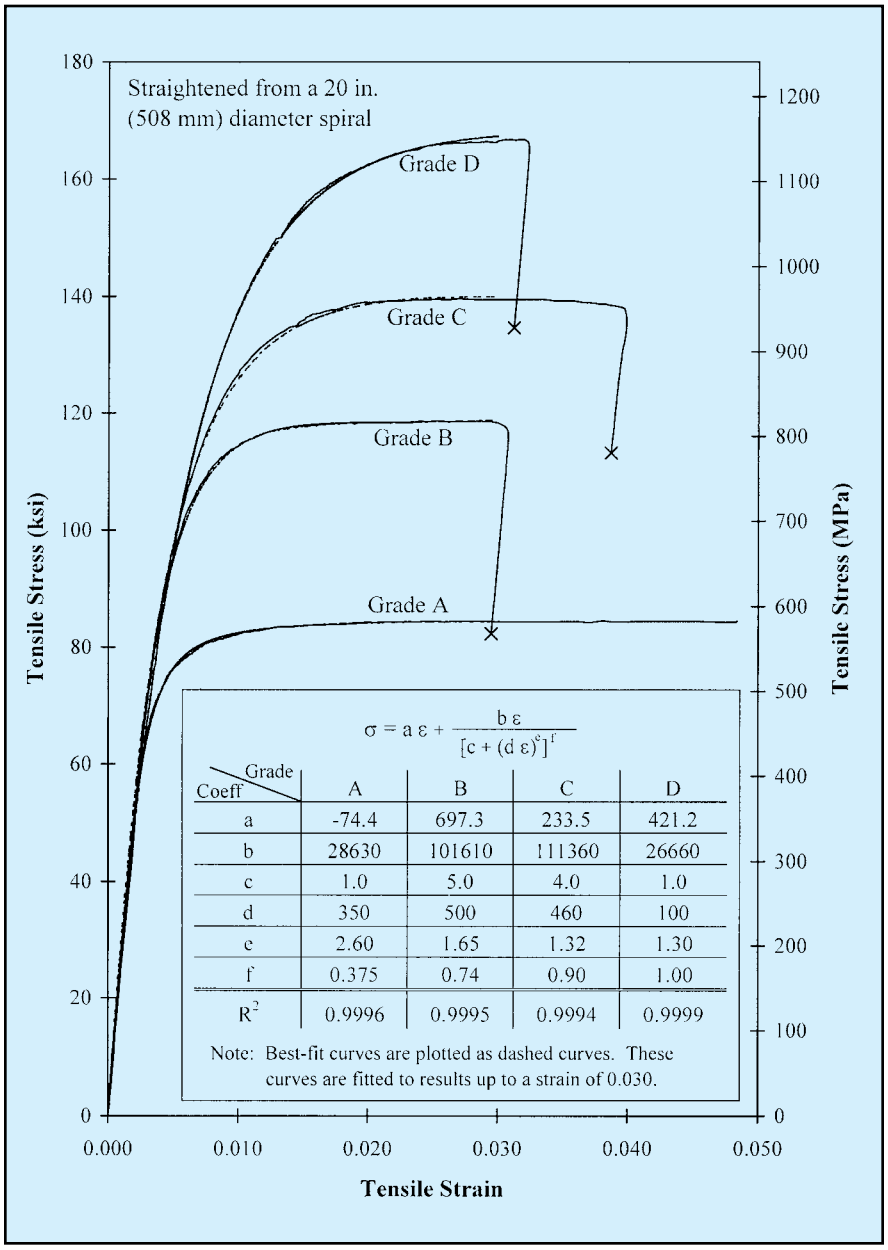

Coeff \ Grade	A	B	C	D
a	-74.4	697.3	233.5	421.2
b	28630	101610	111360	26660
c	1.0	5.0	4.0	1.0
d	350	500	460	100
e	2.60	1.65	1.32	1.30
f	0.375	0.74	0.90	1.00
R^2	0.9996	0.9995	0.9994	0.9999

Fig. 4. Stress-strain behavior of spiraled-straightened steel tested at Lehigh University.

Table 2. Spiral reinforcement properties.

Spiral wire	State of testing	EUL* method yield stress (ksi)	0.2 percent offset yield strain	0.2 percent offset yield stress (ksi)	f_{su} (ksi)	ε_{su}	Data source
A	Unspiraled Straightened	78 –	– 0.0048	– 76	84 85	– > 0.0030	Manufacturer Lehigh
B	Unspiraled Straightened	107 –	– 0.0058	– 102	116 119	– 0.0029	Manufacturer Lehigh
C	Unspiraled Straightened	121 –	– 0.0065	– 109	143 140	– 0.0033	Manufacturer Lehigh
D	Unspiraled Straightened	140 –	– 0.0065	– 111	174 168	– 0.0032	Manufacturer Lehigh

*EUL denotes Elongation Under Load method results from spiral manufacturer.
Note: 1 ksi = 6.895 MPa.

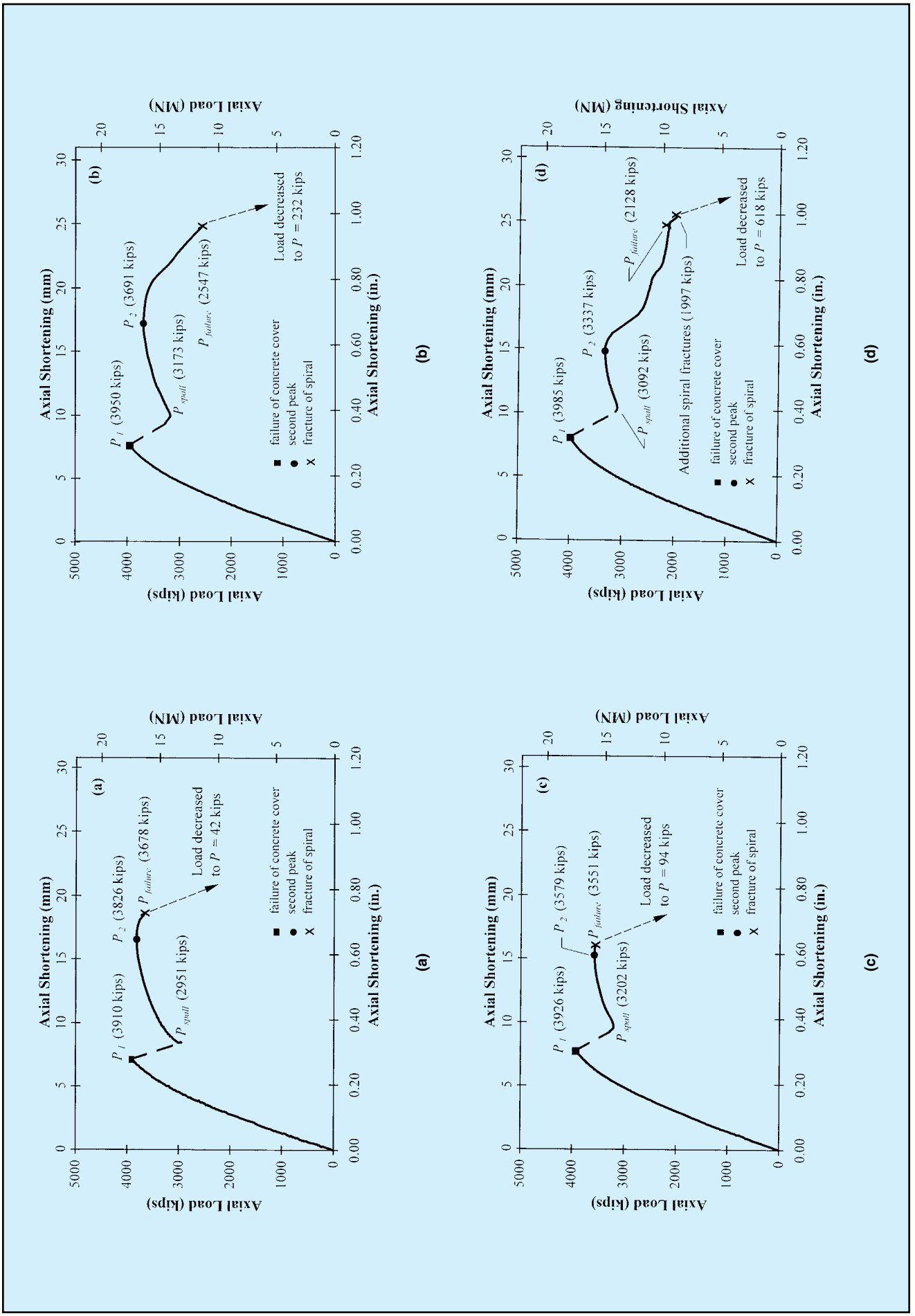

Fig. 5. Plot of axial load versus axial shortening for: (a) Specimen 24-A; (b) Specimen 24-B; (c) Specimen 24-C; (d) Specimen 24-D.

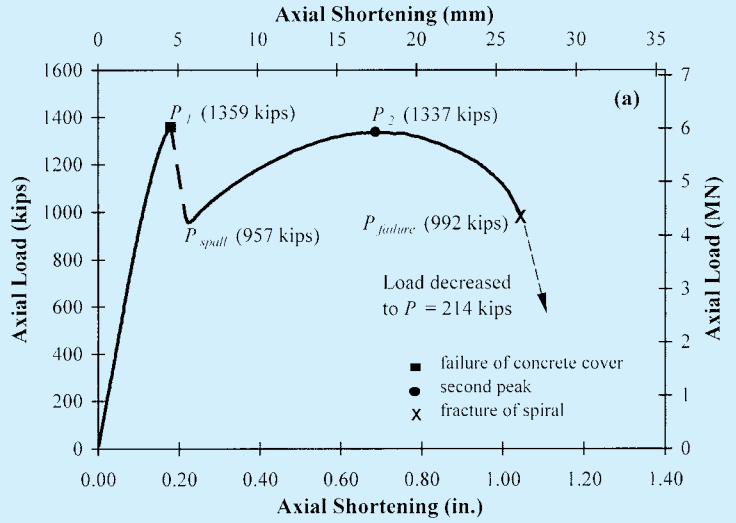

(a)

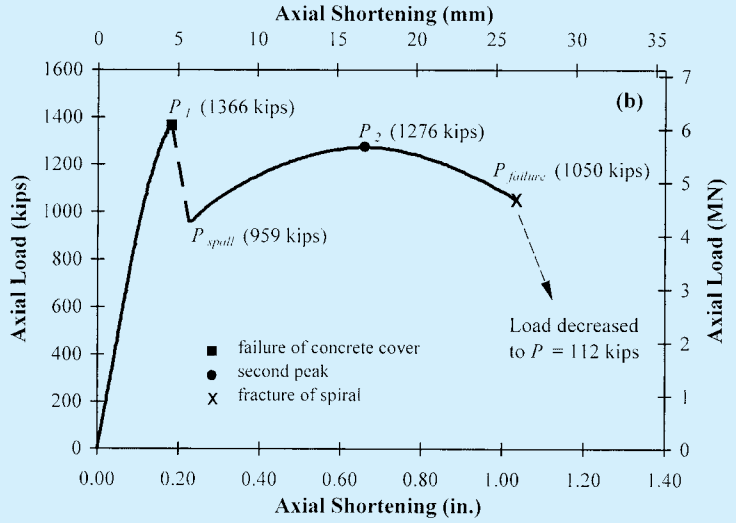

(b)

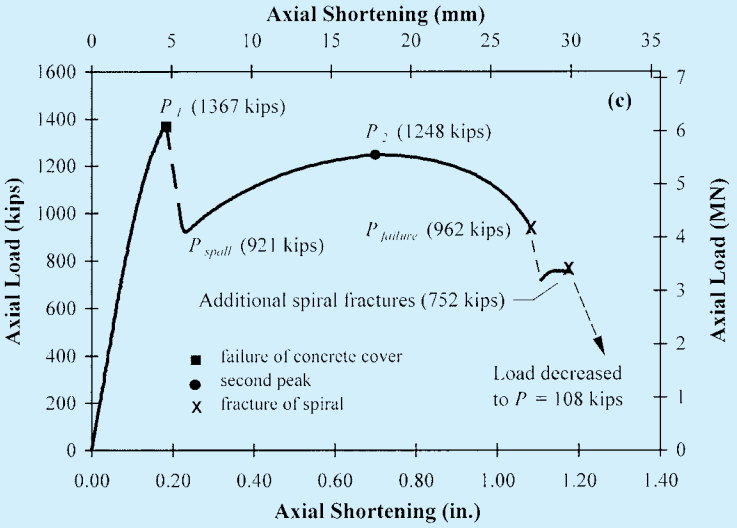

(c)

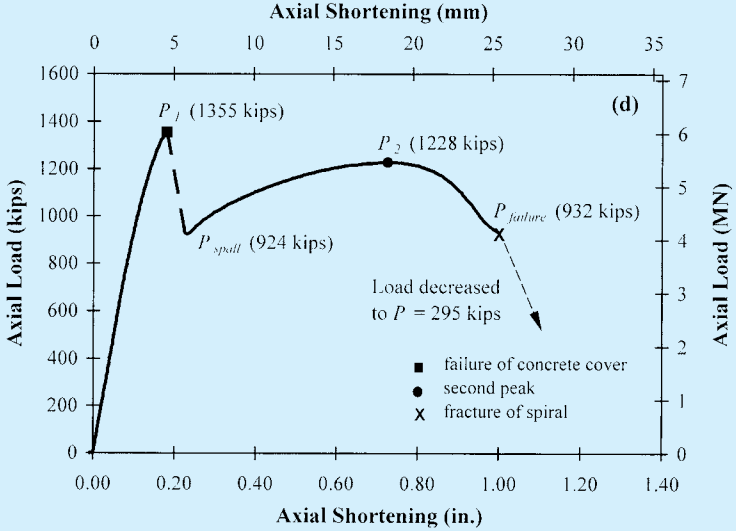

(d)

Fig. 6. Plot of axial load versus axial shortening for: (a) Specimen 14-A; (b) Specimen 14-B; (c) Specimen 14-C; (d) Specimen 14-D.

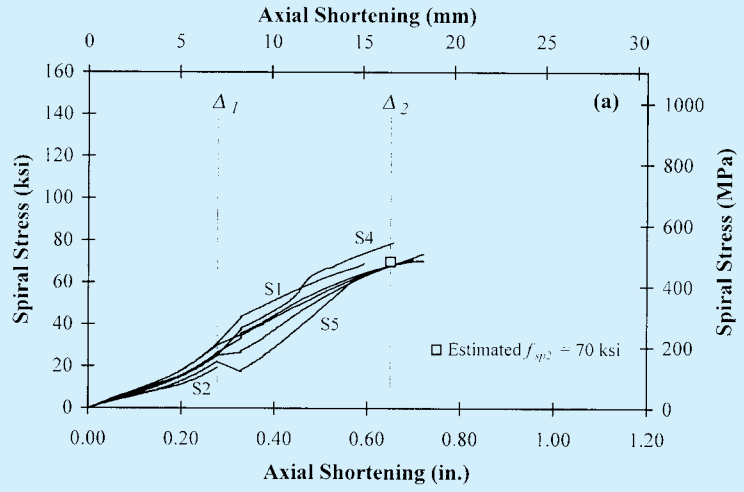

(a)

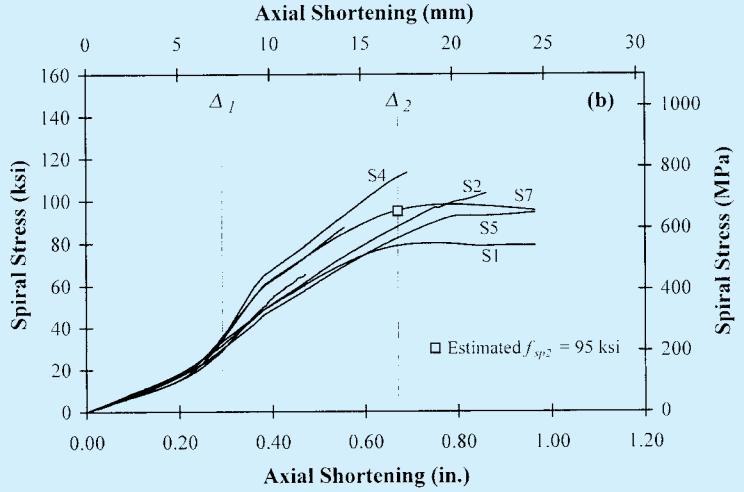

(b)

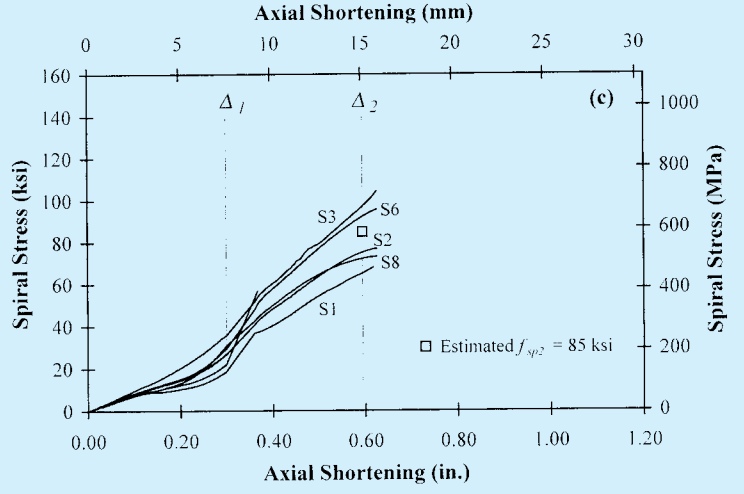

(c)

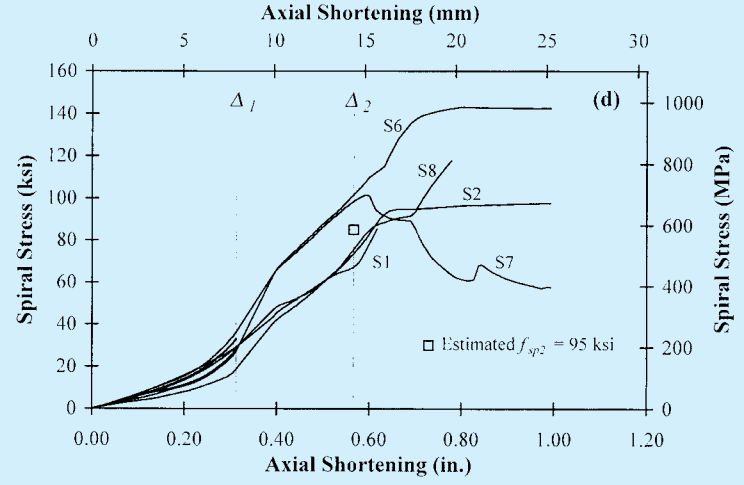

(d)

Fig. 7. Plot of spiral stress versus axial shortening for: (a) Specimen 24-A; (b) Specimen 24-B; (c) Specimen 24-C; (d) Specimen 24-D.

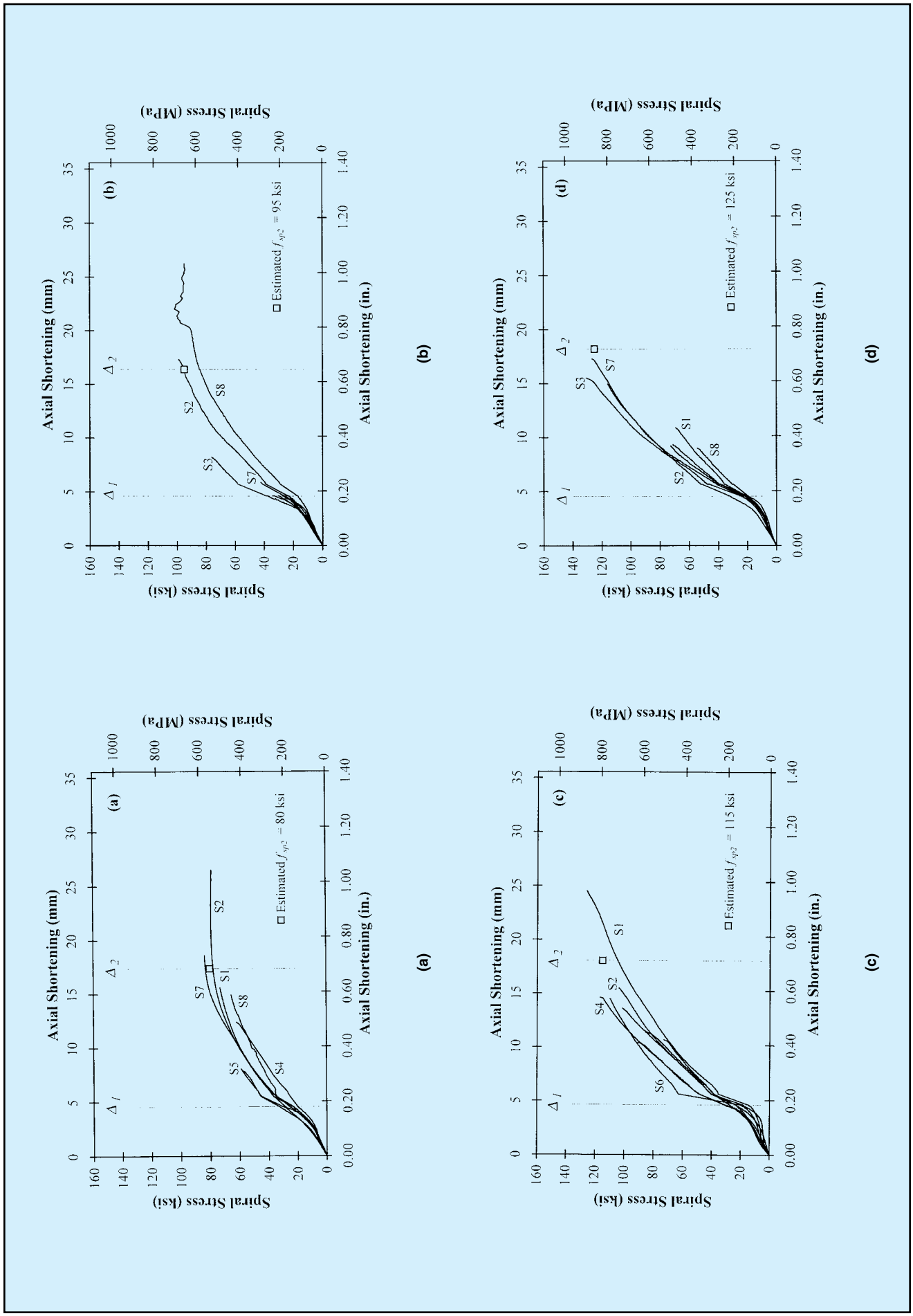

Fig. 8. Plot of spiral stress versus axial shortening for: (a) Specimen 14-A; (b) Specimen 14-B; (c) Specimen 14-C; (d) Specimen 14-D.

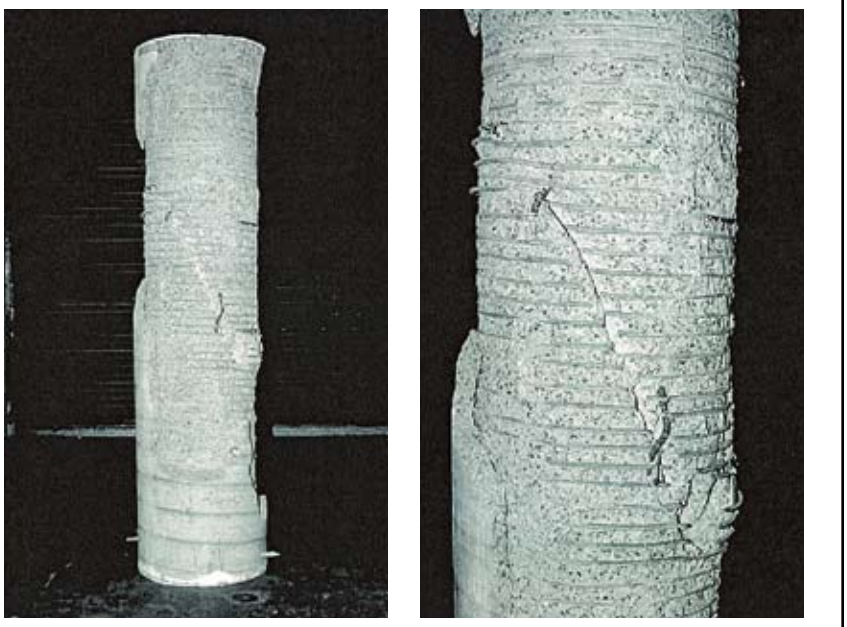

Fig. 9. Post-test appearance of Specimen 24-C: (a) overall view; (b) close-up view of inclined failure plane.

0.2 percent offset method was used to define yield. In this method, the initial modulus of the steel is calculated using stresses from approximately 0 to 25 ksi (0 to 172 MPa). Then, a line with this modulus is drawn on the spiral stress-strain plot beginning at an offset strain of 0.002. The point of intersection between the offset modulus line and the stress-strain curve defines the yield stress and strain.

Table 2 shows that the yield strengths determined from the spiraled-straightened steel tests performed at Lehigh are below the yield strengths determined by the spiral manufacturer. This can be attributed to both the effects of spiraling and straightening on the steel as well as the different methods used to determine yield. The table also provides the ultimate strength of the spiral steel, f_{su}, as well as the corresponding strain, ε_{su}. Note that, as expected, the ultimate strengths of all specimens of each grade are similar.

A best-fit equation was determined for each of the curves shown in Fig. 4. The best-fit equation curves are plotted as dashed lines on Fig. 4 and were fitted for strains between 0.000 and 0.030. The strain value of 0.030 was chosen because the strains measured in the tests were always below this value, and the ultimate strain of each wire as determined from the Lehigh University spiral steel tests was above this value. The figure also shows the equations for the best-fit curves, along with their R^2 value to denote the accuracy of the approximations.

Loading Procedure

Each 24 in. (610 mm) diameter specimen was tested under concentric axial compression in a 5000 kip (22.2 MN) capacity universal testing machine. During the initial portion of a test, the load rate was approximately 70 kips per min. (311 kN per min.), which corresponded to a stress rate of about 155 psi per min. (1069 kPa per min.) and an axial shortening rate of approximately 0.0040 in. per min. (0.102 mm per min.).

Once the desired load rate was achieved during the initial linear portion of the load-shortening behavior, no further adjustments were made to the testing machine. Thus, the actual load rate applied to each specimen decreased due to the softening of the specimen.

The 14 in. (356 mm) diameter specimens were tested in a similar manner as the 24 in. (610 mm) diameter specimens. Through the initial portion of a test, the load rate was about 24 kips per min. (107 kN per min.), which corresponded to a stress rate of about 155 psi per min. (1069 kPa per min.) and an axial shortening rate of approximately 0.0023 in. per min. (0.058 mm per min.).

EXPERIMENTAL RESULTS AND DISCUSSION

Table 3. Approximate stress in spiral reinforcement at Δ_2.

Specimen	$f_{sy,nom}$ (ksi)	Spiral stress		Approximate spiral stress, f_{sp2} (ksi)	Ratio $f_{sp2}/f_{sy,nom}$
		Minimum (ksi)	Maximum (ksi)		
24-A	78	67.7	78.2	70	0.90
24-B	107	78.6	110.4	95	0.89
24-C	121	65.2	97.0	85	0.70
24-D	140	69.5	104.2	85	0.61
14-A	78	70*	82*	80	1.03
14-B	107	85.2	110*	95	0.89
14-C	121	103.4	125*	115	0.95
14-D	140	110*	140*	125	0.89

*Indicates an approximation based on trends observed in data.

Note: 1 ksi = 6.895 MPa; 1 in. = 25.4 mm.

This section of the paper presents the experimental results.

General Axial Load Behavior

Figs. 5 and 6 present plots of axial load versus axial shortening for each specimen. Key axial load values (P_1, P_{spall}, P_2, and $P_{failure}$) are noted on each plot. Figs. 5 and 6 show that each specimen, in general, exhibits the expected axial load-axial shortening behavior shown in Fig. 1, with no noticeable decrease in ductility for the specimens made with the higher strength spirals.

The concrete cover behaved in a similar manner in all eight specimens. In general, the cover failed in a sudden brittle manner when P_1 was reached. No visible damage was observed prior to P_1. The damage which appeared during cover failure included cracks that formed longitudinally as well as circumferentially in the cover concrete. The circumferential cracks were primarily located within the test region of the specimen.

Fig. 9 shows the post-test appearance of Specimen 24-C. Failure of all eight specimens was defined by rupture of one or more turns of wire of the spiral reinforcement and a subsequent loss of confining pressure on the concrete core. This resulted in a significant decrease in the load-carrying capacity of the specimen. However, two observations indicate that the failures were not due to the spiral reinforcement reaching its ultimate strain as caused by lateral expansion of the core.

First, for all specimens, the measured strain in the spiral reinforcement just before failure was less than one-third of the spiral strain at ultimate stress, ε_{su}. Typically, the maximum strains measured during the tests were less than 0.01.

Second, for most of the specimens, multiple spiral fractures occurred simultaneously along a well defined inclined plane throughout the test region. An example of this is shown in Fig. 9(b). This suggests that the plane formed first, and that the spirals fractured as a result of relative movement of the concrete along this plane.

Numerous reports have been published which indicate that high strength concrete [defined here as concrete with a strength above 8 ksi (55 MPa)] fails in confined compression through the formation of an inclined failure plane. Martinez, Nilson, and Slate[10] and Pessiki and Pieroni[11] both have presented findings which pertain specifically to spirally reinforced high strength concrete compression members. Both studies found clearly defined inclined failure planes in the members which contained moderate levels of confinement and high strength concrete.

Martinez et al. reported that the planes that formed in their test specimens were oriented at an angle of approximately 62 degrees from the horizontal. For the larger diameter specimens, the failure plane was clearly defined by both the spiral fractures and the failed concrete. The angle of the plane with the horizontal ranged from 64 to 68 degrees.

For the smaller diameter specimens, the failure plane was only clearly evident in two of the four specimens. The angles of these failure planes were 36 and 41 degrees in Specimens 14-A and 14-C, respectively. It was not clear whether the inclined plane failure mechanism developed in Specimens 14-B or 14-D.

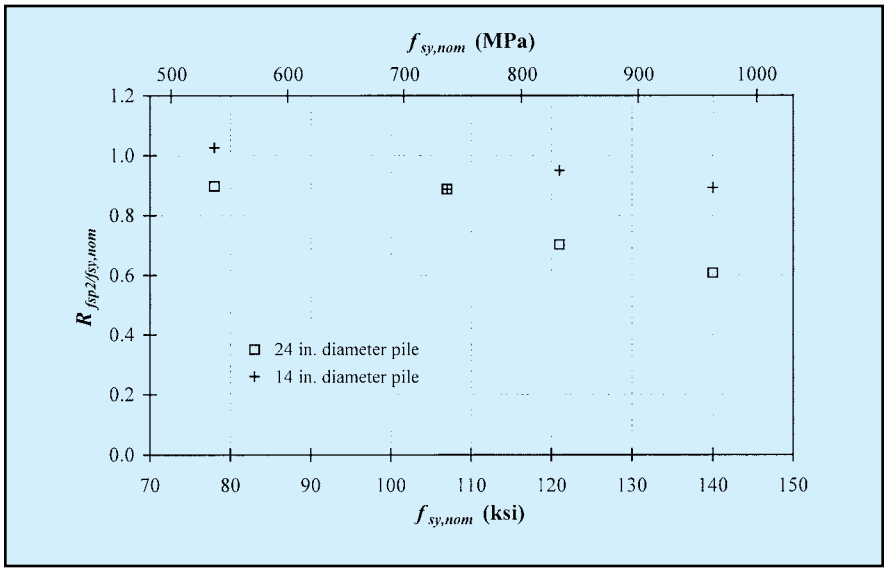

Fig. 10. Ratio of experimentally determined spiral stress at Δ_2, f_{sp2}, to the nominal design spiral yield stress, $f_{sy,nom}$.

Spiral Behavior

Figs. 7 and 8 present plots of spiral stress versus axial shortening for each specimen. The spiral stresses were obtained from the spiral strain measurements and the best-fit stress-strain curves shown in Fig. 4. Results are plotted for each strain gauge up to the point at which the gauge failed. It is noted that the stress-strain curves were obtained from tests of spiraled-straightened wire.

In general, the gauges failed earlier in the 14 in. (356 mm) diameter specimens than in the 24 in. (610 mm) diameter specimens. However, clear trends can be observed from the data collected. In some cases, these trends are used to indicate an approximate range over which the spiral stress most likely lies at key stages in the specimen behavior.

For the compression members treated in this study, the smaller diameter specimens exhibit a larger strain in the spiral reinforcement at the confined concrete peak strength, as compared to the larger diameter specimens.

Table 3 presents the minimum and maximum stresses in the spiral reinforcement at Δ_2. Also presented in this table are values for f_{sp2}, which are single value approximations for the spiral stresses at Δ_2. The values of f_{sp2} are also noted on Figs. 7 and 8 for each individual specimen.

The values of f_{sp2} show that the higher yield strength specimens did reach a high steel stress, but not the design yield stress. The final column of Table 3 shows the ratio of the approximate average spiral stress at Δ_2 to

Table 4. Comparison of experimental peak core concrete strength increase to design value of core concrete strength increase based on assumed yielding of the spiral reinforcement.

Specimen	Experimental			Design			Ratio
	P_2 (kips)	f_{c2} (ksi)	$\Delta f_{c12,exp}$ (ksi)	$f_{sy,nom}$ (ksi)	$f_{2\text{-}2}$ (ksi)	$\Delta f_{c12,dsgn}$ (ksi)	$(\Delta f_{c12})_{exp/dsgn}$
24-A	3826	11.96	3.46	78	0.82	3.36	1.03
24-B	3691	11.52	3.02	107	0.84	3.44	0.88
24-C	3579	11.17	2.67	121	0.79	3.25	0.82
24-D	3337	10.39	1.89	140	0.78	3.21	0.59
14-A	1337	16.46	7.96	78	1.78	7.29	1.09
14-B	1276	15.68	7.18	107	1.80	7.37	0.97
14-C	1248	15.33	6.83	121	1.75	7.19	0.95
14-D	1228	15.07	6.57	140	1.86	7.63	0.86

Note: 1 kip = 4.448 kN; 1 ksi = 6.895 MPa.

the nominal design value of the spiral yield stress. This ratio is also plotted in Fig. 10 versus the nominal spiral yield stress. The ratio of f_{sp2} to $f_{sy,nom}$ ranges from 0.61 to 1.03. In only one case, Specimen 14-A, was f_{sp2} above $f_{sy,nom}$.

Two observations are made from Table 3 and Fig. 10. First, in general, the spirals in the smaller diameter specimens reach a greater fraction of the design yield stress as compared to the spirals in the larger diameter specimens. Second, the stress in the spiral reinforcement is closer to the design yield stress in the lower nominal spiral yield strength specimens. In the higher yield strength specimens, especially for the larger diameter specimens, the stress in the spiral is significantly below the nominal yield value.

Confined Concrete Strength

The axial stress in the concrete core can be estimated from the total axial force carried by the specimen. Of particular interest here is the axial stress in the concrete core at Δ_2. To obtain this stress, the force carried by the longitudinal reinforcement, P_s, is subtracted from the total force carried by the specimen, P_2.

The axial stress in the core is then determined by dividing the remaining force carried by the area of the core concrete, A_{core}. This core area is computed using the out-to-out diameter of the spiral, which is the same definition used by Richart et al. This is expressed in equation form as:

$$f_{c2} = \frac{P_2 - P_s}{A_{core}} \qquad (10)$$

This method of calculating the core concrete stress assumes that the concrete cover carries no axial force after cover failure has occurred.

The experimentally determined increase in the strength of the confined concrete core, $\Delta f_{c12,exp}$, is computed as the stress in the confined core at the second peak, f_{c2}, minus the unconfined compressive strength, f_{co}:

$$\Delta f_{c12,exp} = f_{c2} - f_{co} \qquad (11)$$

In the following paragraphs, the experimentally determined increase in strength of the confined core is compared to the design value of the increase in strength of the confined core, $\Delta f_{c12,dsgn}$, and to the value of the increase in strength of the confined core

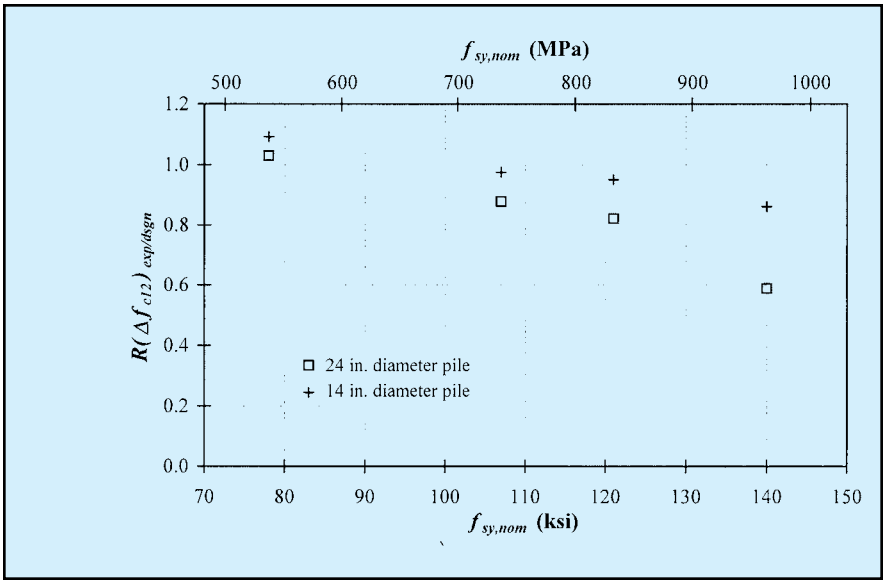

Fig. 11. Ratio of experimental to design Δf_{c12}.

Table 5. Comparison of experimental peak core concrete strength increase to strength increase based on approximate stress in spiral reinforcement at Δ_2.

Specimen	Experimental			Richart et al.[6-8]			Ratio
	P_2 (kips)	f_{c2} (ksi)	$\Delta f_{c12,exp}$ (ksi)	$f_{sy,nom}$ (ksi)	$f_{2\text{-}2}$ (ksi)	$\Delta f_{c12,dsgn}$ (ksi)	$(\Delta f_{c12})_{exp/rich}$
24-A	3826	11.96	3.46	70	0.73	3.00	1.15
24-B	3691	11.52	3.02	95	0.74	3.05	0.99
24-C	3579	11.17	2.67	85	0.55	2.28	1.17
24-D	3337	10.39	1.89	85	0.48	1.95	0.95
14-A	1337	16.46	7.96	80	1.82	7.47	1.07
14-B	1276	15.68	7.18	95	1.60	6.54	1.10
14-C	1248	15.33	6.83	115	1.60	6.54	1.04
14-D	1228	15.07	6.57	125	1.66	6.81	0.96

Note: 1 kip = 4.448 kN; 1 ksi = 6.895 MPa.

calculated from the stress in the spiral reinforcement and the confinement relationship proposed by Richart et al., $\Delta f_{c12,rich}$.

The design value of the increase in strength of the confined core, $\Delta f_{c12,dsgn}$, is calculated from Eq. (12), which is a combination of Eqs. (1) and (6):

$$\Delta f_{c12,dsgn} = 2.05\,\rho_{sp}\,f_{sy,nom} \quad (12)$$

Table 4 shows the experimental and design values for Δf_{c12}. The final column of Table 4 shows the ratio of $\Delta f_{c12,exp}$ to $\Delta f_{c12,dsgn}$. In Fig. 11, this ratio $[R(\Delta f_{c12})_{exp/dsgn}]$ is plotted versus the nominal spiral yield strength of each specimen.

Table 4 and Fig. 11 show that six of the eight specimens did not achieve the level of strength enhancement which was expected based on the spiral design yield strength:

- For the 14 in. (356 mm) diameter specimens, $R(\Delta f_{c12})_{exp/dsgn}$ ranged from 0.86 to 1.09, with Specimens 14-A, 14-B, and 14-C all achieving at least 95 percent of the design strength enhancement.
- For the 24 in. (610 mm) diameter specimens, the ratio ranged from 0.59 to 1.03, with only Specimen 24-A achieving at least 95 percent of the design strength enhancement.
- For both diameter specimens, the strength increase achieved was greater for the specimens with lower yield strength spirals than it was for the specimens with higher yield strength spirals.

The strength increase of the confined core, $\Delta f_{c12,rich}$, calculated from the measured strains in the spiral reinforcement (f_{sp2} in Table 3), is calculated from Eq. (13), which is a combination of Eqs. (1) and (6):

$$\Delta f_{c12,rich} = 2.05\,\rho_{sp}\,f_{sp2} \quad (13)$$

Table 5 shows the experimental and Richart et al. predicted values of Δf_{c12}. The final column of Table 5 shows the ratio of $\Delta f_{c12,exp}$ to $\Delta f_{c12,rich}$. In Fig. 12, this ratio is also plotted versus the nominal spiral yield strength of each specimen. These ratios range from 0.95 to 1.17.

These ratios show that all eight specimens exhibited experimental strength increases consistent with the measured stresses in the spiral reinforcement. Therefore, for the specimens treated in this study, Eq. (1) adequately repre-

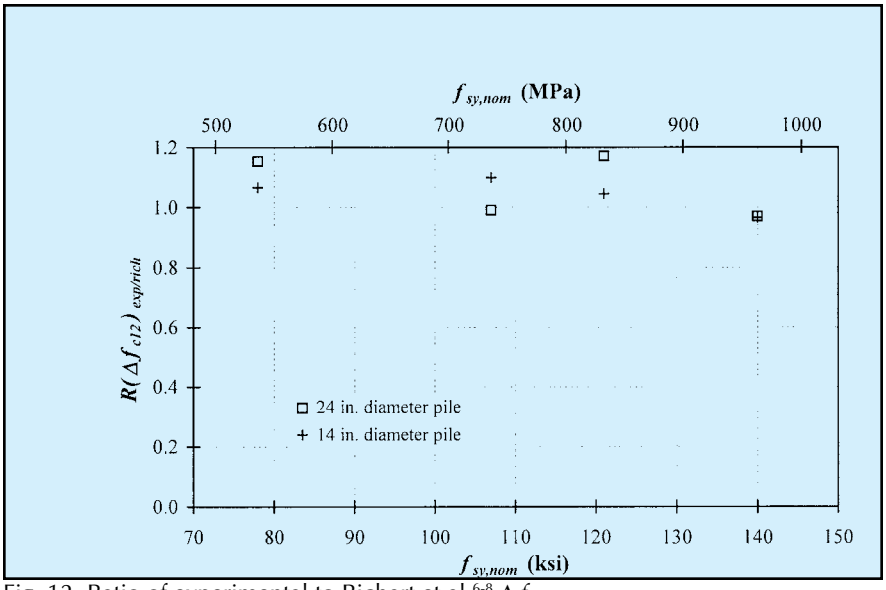

Fig. 12. Ratio of experimental to Richart et al.[6-8] Δf_{c12}.

Table 6. Comparison of experimental longitudinal strain at Δ_2 to value predicted by Richart et al.[6-8]

Specimen	Experimental					Richart et al.	Ratio
	ε_{co}	f_{co} (ksi)	f_{c2} (ksi)	$f_{2\text{-}2}$ (ksi)	ε_{c2}	$\varepsilon_{c2,rich}$	$(\varepsilon_{c2})_{exp/rich}$
24-A	0.0027	8.50	11.96	0.73	0.0088	0.0082	1.07
24-B	0.0027	8.50	11.52	0.75	0.0081	0.0075	1.08
24-C	0.0027	8.50	11.17	0.56	0.0076	0.0069	1.10
24-D	0.0027	8.50	10.39	0.48	0.0093	0.0057	1.64
14-A	0.0027	8.50	16.46	1.82	0.0113	0.0153	0.74
14-B	0.0027	8.50	15.68	1.60	0.0159	0.0141	1.13
14-C	0.0027	8.50	15.33	1.67	0.0183	0.0135	1.36
14-D	0.0027	8.50	15.07	1.66	0.0194	0.0131	1.48

Note: 1 ksi = 6.895 MPa.

sents the relationship between confining pressure and the strength enhancement of the core concrete.

To summarize in general terms, for the specimen geometries and material properties treated in this study, Eq. (1) provides an accurate means of estimating the confined concrete compressive strength, f_{c2}, from the unconfined concrete compressive strength, f_{co}, and the actual confining stress, $f_{2\text{-}2}$. It is emphasized that the equation is accurate only if the actual confining pressure is used. The equation may not provide accurate results if a confining pressure is used which is based on an assumed yield stress in the spiral reinforcement.

Longitudinal Strains

An experimental value of longitudinal strain at Δ_2 was obtained for each specimen from the measurements of strain in the longitudinal steel reinforcement. This value, $\varepsilon_{c2,exp}$, was calculated as the average strain measured in the longitudinal reinforcement at Δ_2.

Table 6 shows the experimentally determined value of longitudinal strain for each specimen. This table shows that, for the specimens treated in this study, the smaller diameter specimens exhibit a larger axial strain at the confined concrete peak strength as compared to the larger diameter specimens.

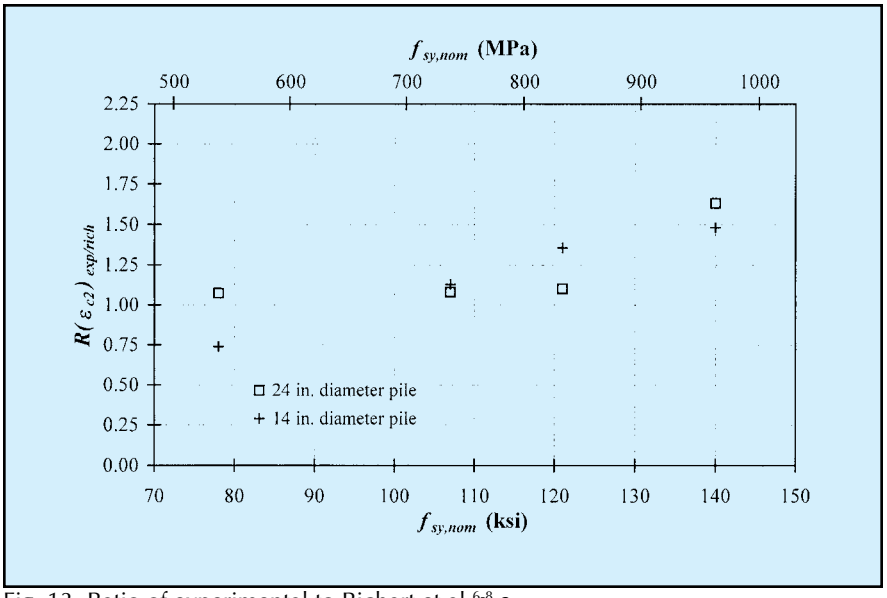

Fig. 13. Ratio of experimental to Richart et al.[6-8] ε_{c2}.

As noted earlier, Eq. (2) was proposed by Richart et al. to predict the axial strain at peak confined compressive strength. The applicability of Eq. (2) was examined by substituting into it the experimentally determined values for ε_{co}, f_{c2}, and f_{co}. The axial strain computed by this equation is referred to as $\varepsilon_{c2,rich}$. The values of ε_{co} and f_{co} were taken as 0.0027 and 8.50 ksi (58.6 MPa), respectively. The value of f_{c2} was determined from Eq. (10).

Table 6 shows the experimentally obtained values and Richart et al. predicted values of ε_{c2}. This table also shows the ratio of the two values, $R(\varepsilon_{c2})_{exp/rich}$. These ratios are also plotted in Fig. 13. In seven of the eight cases, the experimentally observed longitudinal strain is greater than the predicted value.

Additionally, the trend shows that as the value of f_{c2} decreases for a given specimen size (i.e., lower confining pressure), the Richart et al. prediction becomes more conservative. Table 6 and Fig. 13 show that, in general, Eq. (2) provides a reasonable to conservative estimate of the axial strain at the peak compressive stress in the confined core.

DESIGN IMPLICATIONS

The test results presented in this paper demonstrate that spiral steel stresses in excess of 60 ksi (414 MPa) may be achieved in spirally-reinforced compression members. However, the tests also indicate that the yield stress of the spiral may not be achieved. Thus, while design stresses greater than 60 ksi (414 MPa) may be possible, the design stress may not simply be taken as the yield stress for these higher strength spirals.

The reason for this is that the actual stress reached in the spiral depends in part upon the compression member diameter, with smaller diameter compression members able to reach a greater fraction of the design yield stress as compared to the larger diameter compression members. For a given concrete cover thickness, these smaller diameter members have a greater volume fraction of spiral reinforcement as compared to larger diameter members. What is needed for design is a method to determine what level of stress can be reached by a given spiral wire in a particular combination of compression member geometry and material properties.

Based on the test results presented in this paper, a procedure has been proposed for the design of high strength spiral reinforcement.[3,4] In the proposed procedure, the design of the spiral is based on the determination of a *useable stress* for a given spiral wire, rather than the yield stress of the wire. This procedure has been evaluated in a series of tests reported elsewhere.[12,13]

CONCLUSIONS

The following conclusions are made based on the research presented in this paper. The conclusions apply to the specimen geometries and material properties treated in this study:

1. Spiral stresses in excess of 60 ksi (414 MPa) may be achieved in spirally-confined compression members. Thus, the current code provisions that limit the design yield strength of spiral reinforcement in compression members to 60 ksi (414 MPa) may be overly conservative.

2. For a given concrete cover thickness, smaller diameter compression members exhibit a larger axial strain at the confined concrete peak strength and a larger strain in the spiral reinforcement at the confined concrete peak strength, as compared to the larger diameter compression members. Accordingly, the spirals in the smaller diameter compression members reach a greater fraction of the design yield stress as compared to the spirals in the larger diameter compression members. Also, in general, the stress in the spiral reinforcement is closer to the design yield stress in the lower nominal spiral yield strength specimens.

3. Eq. (1) provides an accurate means of estimating the confined concrete compressive strength, f_{c2}, from the unconfined concrete compressive strength, f_{co}, and the actual confining stress, $f_{2\text{-}2}$. It is emphasized that the equation is accurate only if the actual confining pressure is used. The equation may not provide accurate results if a confining pressure is used which is based on an assumed yield stress in the spiral reinforcement.

4. Eq. (2) provides a reasonable to conservative estimate of the axial strain at the peak compressive stress in confined concrete.

5. Compression members made with high strength reinforcement exhibit the expected axial load-axial shortening behavior shown in Fig. 1, with no noticeable decrease in ductility for the specimens made with the higher strength spirals.

6. Failure of all specimens was precipitated by the failure of the concrete and not of the spiral steel. Evidence to support this conclusion includes the observation that all spiral steel strains were well below the fracture strains for the spirals when specimen failure occurred, and that in most instances the spiral fractured along a well-defined inclined failure plane.

ACKNOWLEDGMENTS

This investigation was funded by the Precast/Prestressed Concrete Institute, through a Daniel P. Jenny Fellowship, and by the Center for Advanced Technology for Large Structural Systems (ATLSS).

Additional support was provided by Bayshore Concrete Products Corporation, Concrete Technology Corporation, Florida Wire and Cable, Inc., Morse Bros., Inc., Sumiden Wire

Products Corporation, and Utility Vault Company, Inc. Support from the sponsors is gratefully acknowledged.

The authors also thank Stephen Seguirant, James Iverson, Saad Moustafa, and McLeod Nigels for their careful reviews of the paper.

The findings and conclusions presented in this paper are those of the authors, and do not necessarily reflect the views of the sponsors or the individuals acknowledged above.

REFERENCES

1. ACI Committee 318, "Building Code Requirements for Structural Concrete (ACI 318-95) and Commentary (ACI 318R-95)," American Concrete Institute, Farmington Hills, MI, 1995.
2. AASHTO, *AASHTO LRFD Bridge Design Specifications*, American Association of State Highway and Transportation Officials, Washington, D.C., First Edition, 1994.
3. Graybeal, B. A., "Confinement Effectiveness of High Strength Spiral Reinforcement in Prestressed Concrete Piles," M.S. Thesis, Department of Civil and Environmental Engineering, Lehigh University, Bethlehem, PA, May 1998, 228 pp.
4. Graybeal, B., and Pessiki, S., "Confinement Effectiveness of High Strength Spiral Reinforcement in Prestressed Concrete Piles," Report No. 98-01, Center for Advanced Technology for Large Structural Systems, Lehigh University, Bethlehem, PA, April 1998, 168 pp.
5. Considère, A., "Rèsistance à la compression du bèton armè et du bèton frettè," *G nie Civil*, Paris, France, 1903.
6. Richart, F. E., Brandzaeg, A., and Brown, R.L., "A Study of the Failure of Concrete Under Combined Compressive Stresses," *University of Illinois Bulletin*, V. 26, No. 12, November 20, 1928, 104 pp.
7. Richart, F. E., Brandzaeg, A., and Brown, R.L., "The Failure of Plain and Spirally Reinforced Concrete in Compression," *University of Illinois Bulletin*, V. 26, No. 31, April 2, 1929, 74 pp.
8. Richart, F. E., Brandzaeg, A., and Brown, R. L., "An Investigation of Reinforced Concrete Columns," *University of Illinois Bulletin*, V. 31, No. 40, June 5, 1934, 94 pp.
9. *PCI Design Handbook – Precast and Prestressed Concrete*, Fifth Edition, Precast/Prestressed Concrete Institute, Chicago, IL, 1999.
10. Martinez, S., Nilson, A. H., and Slate, F. O., "Spirally Reinforced High-Strength Concrete Columns," *ACI Journal*, V. 81, No. 5, September-October 1984, pp. 431-442.
11. Pessiki, S., and Pieroni, A. M., "Axial Load Behavior of Large-Scale Spirally-Reinforced High-Strength Concrete Columns," *ACI Structural Journal*, V. 94, No. 3, May-June 1997, pp. 304-314.
12. Mudlock, M., "Design of High

APPENDIX — NOTATION

A_{core} = core concrete area measured to outside diameter of spiral
A_g = gross cross-sectional area
A_{sp} = total cross-sectional area of bundled spiral wires
A_{st} = total area of longitudinal reinforcement
d_{sp} = diameter of spiral measured out-to-out of wire
d_{sw} = diameter of an individual spiral wire
$f_{2\text{-}2}$ = lateral confining stress exerted on confined concrete at Δ_2
f_{c2} = compressive strength of confined concrete at Δ_2
f_{co} = compressive strength of unconfined concrete
f_{pc} = concrete compressive stress due to effective prestress
f_{sp} = stress in spiral reinforcement
f_{sp2} = stress in spiral reinforcement at Δ_2
f_{su} = ultimate strength of spiral reinforcement
f_{sy} = yield strength of spiral reinforcement
$f_{sy,nom}$ = nominal yield strength of spiral reinforcement as reported by spiral manufacturer
f_y = yield strength of longitudinal reinforcement
n_{sp} = number of spiral wires bundled to form a single turn of spiral
P_1 = axial load just prior to cover spalling
P_2 = axial load at Δ_2
$P_{failure}$ = axial load at failure
P_o = nominal axial load capacity
P_s = axial force carried by longitudinal reinforcement
P_{spall} = lowest axial load between Δ_1 and Δ_2
$R_{fsp2/fsy,nom}$ = ratio of spiral stress at Δ_2 to nominal design spiral yield stress
$R(\Delta f_{c12})_{exp/dsgn}$ = ratio of experimental to design increase in concrete stress from Δ_1 to Δ_2
$R(\Delta f_{c12})_{exp/rich}$ = ratio of experimental to Richart et al. predicted increase in concrete stress from Δ_1 to Δ_2
$R(\varepsilon_{c2})_{exp/rich}$ = ratio of experimental to Richart et al. predicted longitudinal strain at Δ_2
s = spiral pitch
Δf_{c12} = change in confined core stress between Δ_1 and Δ_2
Δ_1 = axial shortening corresponding to P_1
Δ_2 = axial shortening corresponding to P_2
Δ_{spall} = axial shortening corresponding to P_{spall}
$\Delta_{failure}$ = axial shortening corresponding to $P_{failure}$
ε_{c2} = axial strain in concrete corresponding to f_{c2}
ε_{co} = axial strain in concrete corresponding to f_{co}
ε_{su} = strain in spiral reinforcement corresponding to f_{su}
ε_y = strain in reinforcement corresponding to f_y
ρ_{lg} = ratio of area of longitudinal reinforcement to total area of concrete in section (A_g)
ρ_{sp} = ratio of volume of spiral reinforcement to total volume of core (A_{core})